doi: 10.82124/CEAS-GNC-2026-028 CEAS-GNC-2026-028

A Reference Model Architecture with Pseudo Control Hedging for Actuator Saturation in Transition Aircraft

Sinan Çimen Research Associate, University of Stuttgart, Institute of Flight Mechanics and Controls, 70569, Stuttgart, Germany. sinan.cimen@ifr.uni-stuttgart.de

Manuel Storrer Research Associate, University of Stuttgart, Institute of Flight Mechanics and Controls, 70569, Stuttgart, Germany. manuel.storrer@ifr.uni-stuttgart.de

Walter Fichter Professor, University of Stuttgart, Institute of Flight Mechanics and Controls, 70569, Stuttgart, Germany. fichter@ifr.uni-stuttgart.de

ABSTRACT

Designing a reference model that produces trajectories reflecting capabilities of the aircraft is crucial for control system design. Fundamentally, it offers two advantages. First, it prevents integrator windup when there is an integral action in the controller. Second, it mitigates actuator saturation and reduces the effect of unachievable commands on other axes, in the case of multi-axis effectors like propellers in a multi-rotor aircraft. Pseudo control hedging (PCH) provides a feedback of the unachieved pseudo controls to the reference model, in order to slow down reference trajectories. Typically, implementation of PCH alters the closed-loop response of the system, since it accounts for not only actuator nonlinearities like saturations, but also the linear dynamics of the actuators. Moreover, in feedforward-feedback control structures, the effect of hedging is not visible in the pseudo control command unless reference model is significantly slower than the controller. In this paper, we propose a PCH structure that is active only in the case of actuator saturations and therefore, does not alter the nominal closed-loop response and does not require the reference model to be slower than the controller. Additionally, we propose a reference model architecture with a novel PCH implementation for a transition aircraft employing a unified control strategy.

Keywords: Reference Model, Pseudo Control Hedging, Flight Control, Unified Control

1 Introduction

In control system design, computing physically feasible reference trajectories plays a crucial role. Reference models in flight control systems receive inputs from the pilot or from the outer loop controller, and produce a feasible reference signal to the respective controllers. The aim for the design of the reference model is to produce trajectories that are realizable by the aircraft, and the bandwidth of the reference model is as high as possible in order to preserve agility of the aircraft. However, the upper limit of the bandwidth of the reference model is limited by the bandwidth of the corresponding control loop, since a dynamical system is not expected to track a reference signal that is faster than its capabilities.

Pseudo control hedging (PCH) is a way of compensating the reference model for the unaccounted actuator dynamics [1]. These actuator dynamics can include nonlinear effects such as position and rate limits, and also the linear dynamics of the actuator. First, the difference between pseudo control command and an approximation of the achieved pseudo controls based on measured or estimated actuator position

is computed. Then, the internal dynamics of the reference model is slowed down by that difference. This method is applied to several types of flight control systems, such as adaptive control [2, 3], nonlinear dynamic inversion (NDI) [4] and incremental nonlinear dynamic inversion (INDI) [5].

Since the classical PCH approach also accounts for linear actuator dynamics, it modifies the nominal closed-loop response of the system, even when there is no nonlinear effect active on the actuator. This may not be desired because linear dynamics of the actuator could be already taken into account in the controller gain design phase, by separating the bandwidth of the innermost control loop and the bandwidth of the actuator sufficiently. Several designs include a modified version of PCH that only considers actuator saturations, by computing achieved pseudo controls resulting from actuator commands limited by the actuator limits [6]. In this work, we adopt an identical version of computing the achieved pseudo control.

Control of transition aircraft using unified control approaches such as INDI requires a closer examination of the reference models, since multiple flight phases come with different physical capabilities. Existing approaches in the literature include applying a simple low-pass filter to pilot commands [7], using linear reference models with pseudo control feedforward [8] and employing cascaded NDI-based reference models [5]. A review of reference models used with INDI control laws is presented in [9]. For command filtering and linear reference models, there is a need of phase-dependent modification of the reference model, such as limiting the derivatives of the reference depending on the flight phase or applying PCH to slow down the reference model. Otherwise, they have to be slow enough to provide physically feasible trajectories across all flight phases. This, however, can lead to an overly conservative reference model and, as a result, loss of agility for the aircraft. NDI-based approaches can provide this phase-dependent behavior, since they compute dynamical limits of the aircraft at each timestep. However, since they rely on the model of the aircraft, they remove the key advantage of INDI of being independent of extensive model knowledge. Considering these, linear reference models in combination with PCH become advantageous since they do not require additional model knowledge, and can modify the reference trajectories in case of actuator saturations. In this work, we propose a novel reference model architecture for unified control of transition aircraft, using linear reference models with PCH.

In control structures without a feedforward command from the reference model, hedging slows down the reference and hence decreases the pseudo control command with a signal that is equal to the low-pass filtered hedging signal. However, in linear feedforward-feedback structures, when the reference model and the error controller bandwidths match, pseudo control command stays the same as in the case with no hedging, since the changes in the reference signal and the feedforward contribution cancel each other. In the case where reference model is slower than the error controller, hedging mitigates saturations by decreasing pseudo control command. However, the steady-state gain of this effect depends on the ratio between reference model and error controller bandwidths. [6] proposed a gain on the hedging signal for linear feedforward-feedback structures in order to make the steady-state gain of the effect of the hedging signal on the pseudo control command always one. However, the gain can result in non-physical reference trajectories and hence can result in windup in the case of an integral action within controllers. For linear feedforward-feedback structures, we propose a new hedging structure, which enables fast reference models with bandwidths similar to those of error controllers, while keeping the contribution of the hedging signal to the pseudo control command as a low-pass filtered signal with steady-state gain of one.

This paper discusses a comparison of reference models with different hedging augmentations in Section 2. The proposed reference model architecture for unified control approaches is given in Section 3. Several simulations are performed on a transition aircraft model to highlight the advantage of the proposed architecture with comparisons to unhedged case and results are given in Section 4. Remarks and conclusions are given in Section 5.

2 Analysis of Pseudo Control Hedging

An example INDI control architecture with PCH is given in Fig. 1. In the figure, ν_h represents the hedging signal, B is the control effectiveness matrix, ν_{cmd} is the total pseudo control command consisting of feedforward term from reference model $\nu_{\text{cmd,ff}}$ and feedback term $\nu_{\text{cmd,fb}}$. Allocation outputs an incremental actuator command Δu_{cmd}, while considering actuator limits $\overline{u}$ and $\underline{u}$. $\hat{y}$ and $\hat{\nu}$ are state and pseudo control estimate, respectively. This architecture differs from most of the architectures in the literature with PCH, since it computes the hedging signal as the difference between incremental pseudo control command and realized pseudo control command based on the output of the allocation, similar to [6]. Therefore, actuator dynamics are not considered in the calculation of hedging signal. Only the saturation of the actuators triggers the hedging signal ν_h and it is zero in case of nominal operations without saturated actuators. The closed-loop response remains unchanged for pseudo control commands that are inside the attainable moment set (AMS).

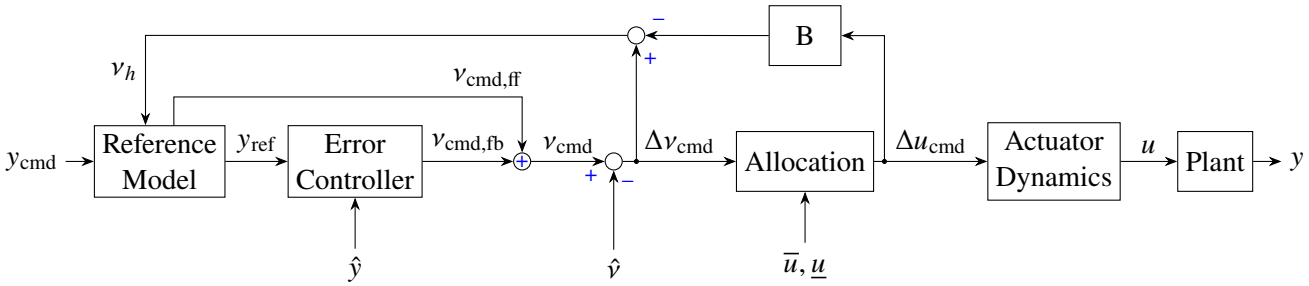

Fig. 1 Example control architecure with PCH and baseline INDI controller.

A linear reference model for a control loop with relative degree of r and filter order of n is given in Fig. 2. y_{ref}^i is the i-th derivative of the reference y_{ref}. For a control system, it is expected that filter order is selected such that $n \geq r$, since the underlying dynamical system has at least an order of r. In case of additional dynamics that are not considered in the dynamic inversion, such as actuator dynamics, the order of the underlying dynamics becomes higher than the relative degree.

The hedging signal ν_h is computed as

$$\nu_h = \nu_{\text{cmd}} - \hat{\nu}, \tag{1}$$

where pseudo control estimate $\hat{\nu}$ can be estimated using state estimate $\hat{x}$ and actuator commands u_{cmd}. When the baseline controller is INDI, both pseudo control command to the allocation and actuator commands take incremental form and state-dependent terms can be neglected in accordance with the time-scale separation assumption [10]:

$$\nu_h = \Delta\nu_{\text{cmd}} - B\Delta u_{\text{cmd}}. \tag{2}$$

2.1 Pseudo Control Hedging with Feedback Controller

A first order reference model with hedging, which generates reference for a P controller, is given in Fig. 3. k_e is the gain of the controller and k_r is the gain of the reference model. Note that, the underlying dynamical system is assumed to have a relative degree of 1, so that hedging signal is at the same algebraic level as the derivative of the reference. The derivative of the reference is

$$\dot{y}_{\text{ref}} = k_r \left(y_{\text{cmd}} - y_{\text{ref}}\right) - \nu_h. \tag{3}$$

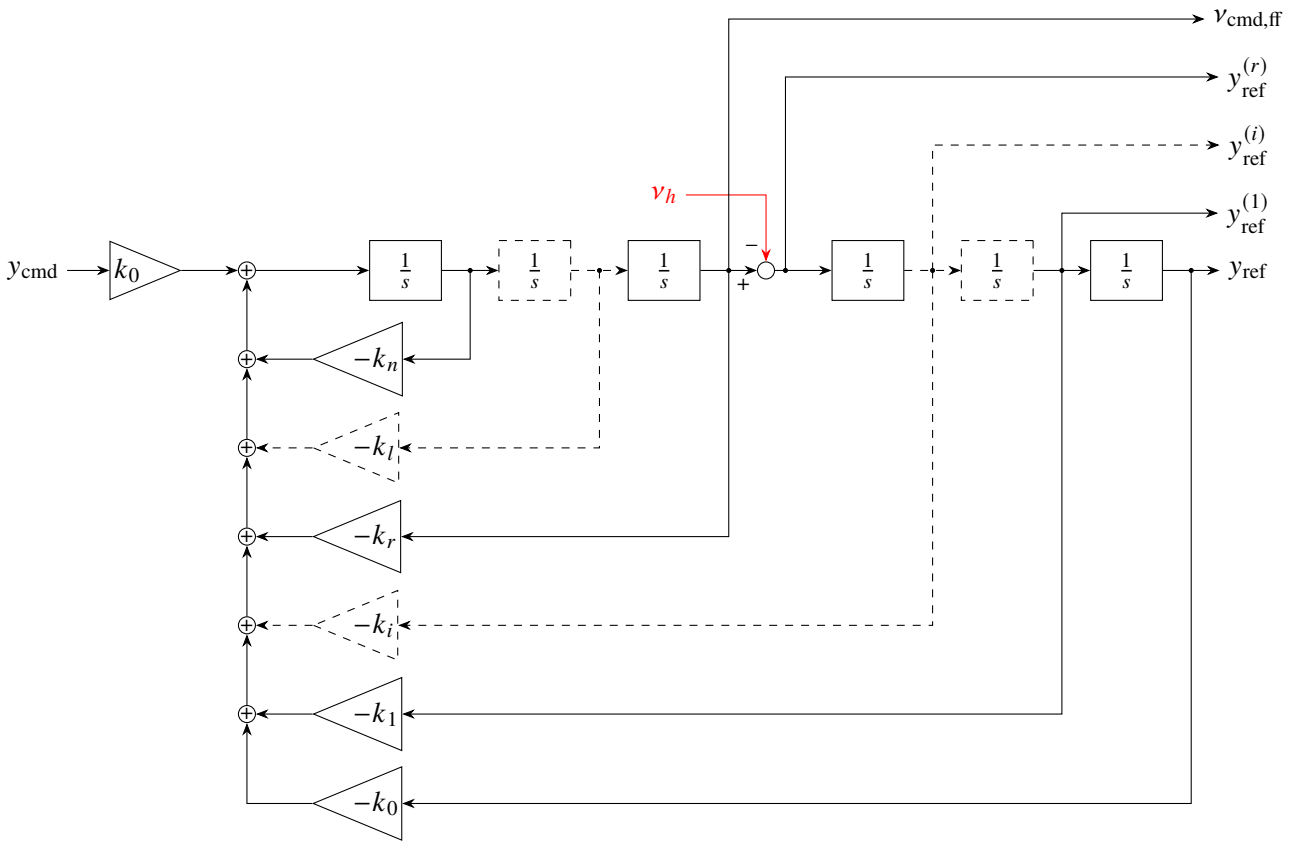

Fig. 2 A generic linear reference model with PCH.

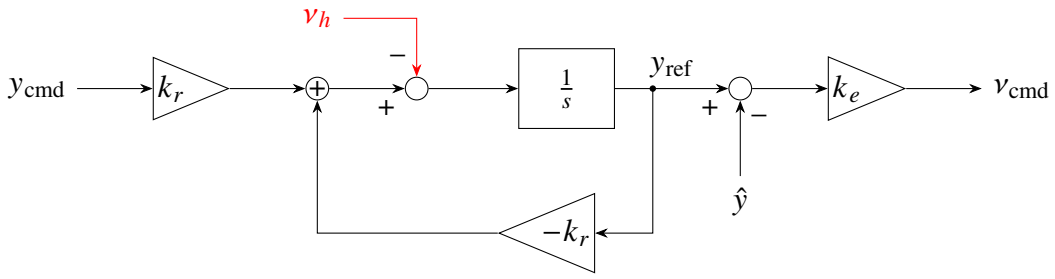

Fig. 3 First order reference model with PCH and P controller.

The reference signal y_{ref} and pseudo control command ν_{cmd} are

$$y_{\text{ref}} = \frac{y_{\text{cmd}} k_r - \nu_h}{s + k_r} \quad \text{and} \tag{4}$$

$$\nu_{\text{cmd}} = (y_{\text{ref}} - \hat{y})\, k_e = \left(\frac{y_{\text{cmd}} k_r}{s + k_r} - \hat{y} \right) k_e - \frac{\nu_h k_e}{s + k_r}. \tag{5}$$

A positive hedging signal always has a low-pass filtered slow-down effect on reference signal y_{ref}, as it can be seen from Eq. 4. Therefore, hedging improves the tracking performance in case of saturations by slowing down the reference model. Moreover, hedging signal again has a low-pass filtered slow-down effect on pseudo control command ν_{cmd}, as in Eq. 5, with a steady-state gain of k_e/k_r, which results in mitigating actuator saturations.

2.2 Pseudo Control Hedging with Feedforward-Feedback Controller

A first order reference model with feedforward-feedback control structure is given in Fig. 4. The underlying dynamical system is assumed to have a relative degree of 1, so that hedging signal affects the derivative of the reference signal.

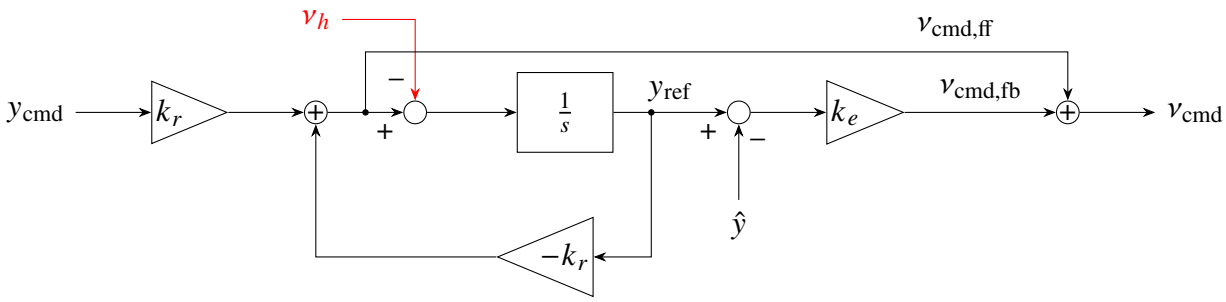

Fig. 4 First order reference model with PCH and feedforward-feedback control.

The effect of hedging on the reference signal is the same as feedback-only control case, as in Eq. 4. The pseudo control command includes both feedback and feedforward term:

$$\nu_{\text{cmd}} = \nu_{\text{cmd,fb}} + \nu_{\text{cmd,ff}}, \tag{6}$$

where contribution of feedback control $\nu_{\text{cmd,fb}}$ is the same as Eq. 5. The feedforward term $\nu_{\text{cmd,ff}}$ can be written as:

$$\nu_{\text{cmd,ff}} = k_r \left(y_{\text{cmd}} - y_{\text{ref}}\right) = k_r \left(y_{\text{cmd}} - \frac{y_{\text{cmd}} k_r - \nu_h}{s + k_r}\right) = \frac{y_{\text{cmd}} k_r}{s + k_r} s + \frac{\nu_h k_r}{s + k_r}. \tag{7}$$

From Eq. 7, it can be seen that hedging signal has an add-on effect on feedforward pseudo control term, $\nu_{\text{cmd,ff}}$. Combining Eq. 5 and 7, the total pseudo control command ν_{cmd} becomes:

$$\nu_{\text{cmd}} = \left(\frac{y_{\text{cmd}} k_r}{s + k_r} - \hat{y}\right) k_e + \frac{y_{\text{cmd}} k_r}{s + k_r} s - \frac{\left(k_e - k_r\right) \nu_h}{s + k_r}, \tag{8}$$

where the first term corresponds to the unhedged feedback pseudo control contribution, and the second terms corresponds to the unhedged feedforward pseudo control contribution. The last part shows the effect of hedging signal ν_h on total pseudo control command. From the rightmost term of Eq. 8 and also as shown in [6], it is visible that a positive hedging signal has a decreasing effect on pseudo control command, if $k_e > k_r$. In case the reference model and the error controller have the same gain, $k_e = k_r$, then the effect of hedging on pseudo control command is vanished. In case the reference model is faster than the error controller, $k_r > k_e$, hedging signal will add-on to the pseudo control command, which is undesirable since it leads to greater saturations.

Even when the error controller is faster than the reference model, $k_e > k_r$, the effect of hedging on pseudo control command has a steady-state gain of $(k_e - k_r)/k_r$. Normally, it is desired to have a steady-state gain of one since both pseudo control command and hedging signal are on the same algebraic level. [6] proposed a scaling gain K_h on hedging signal to ensure that steady-state gain of the effect of hedging on pseudo control command is always one, whenever $k_e > k_r$. Such a scaling ensures the desired pseudo control response of the system, however it comes with two disadvantages. First, the method still needs the reference model to be slower than the error controller, which can be undesirable for many use cases where a fast response is required and the error controller bandwidth is limited because of low actuation bandwidth or low sensor bandwidth. Second, when k_r and k_e get close to each other, the scaling gain of the hedging K_h increases. A higher K_h results in higher effect of hedging signal ν_h on reference signal

y_{cmd}, as seen in Eq. 4. This can result in a non-physical reference signal, and therefore, a lower tracking performance. In case of a controller with integral action, the system response may degrade because of a non-physical reference signal. Several simulations of such a scaling on a first-order system with P and PI controllers are shown later in this chapter.

Although the benefit of PCH on pseudo control command in feedforward-feedback control case depends on the relation between the reference model gain k_r and the error controller gain k_e, the benefit in terms of slowing down the reference signal y_{cmd} and having better tracking performance does not depend on how k_r and k_e are chosen. Also, scaling requires the reference model to be slower than the error controller and may result in non-physical reference trajectories. To overcome these issues, a novel structure is proposed that separates the reference signal and feedforward pseudo control. The reference signal is computed from a hedged reference model as in Fig. 4 and the feedforward pseudo control is computed from an unhedged reference model to get rid of canceling effect of feedforward and feedback contributions of hedging signal when $k_e = k_r$, and avoid using a scaling on the hedging signal. The proposed structure is given in Fig. 5.

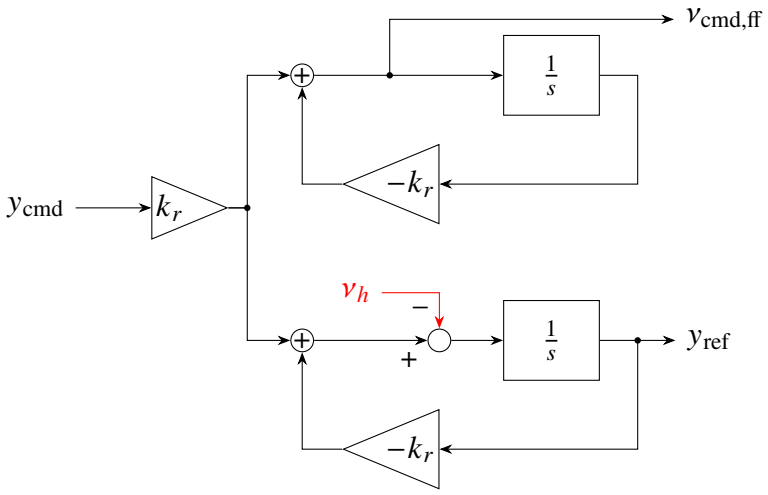

Fig. 5 First order hedged reference model in the proposed structure.

The proposed structure yields the reference signal given in Eq. 4, a total pseudo control command consisting of Eq. 5 and unhedged feedforward terms, such that:

$$\nu_{\text{cmd}} = \left(\frac{y_{\text{cmd}} k_r}{s + k_r} - \hat{y} \right) k_e + \frac{y_{\text{cmd}} k_r}{s + k_r} s - \frac{k_e \nu_h}{s + k_r}. \tag{9}$$

In case the reference model gain and the error controller gain are equal, $k_e = k_r$, Eq. 9 becomes:

$$\nu_{\text{cmd}} = \left(\frac{y_{\text{cmd}} k_r}{s + k_r} - \hat{y} \right) k_r + \frac{y_{\text{cmd}} k_r}{s + k_r} s - \frac{k_r \nu_h}{s + k_r}, \tag{10}$$

which shows that hedging signal effect has a steady-state gain of one and filtered through a low-pass filter with cutoff frequency k_r.

Four different first order reference model schemes are compared for the closed-loop system with first order dynamics and P controller. Plant transfer function is $P(s) = 1/s$, error controller and reference model gains are $k_e = k_r = 1$. Pseudo control saturation limit is assumed to be $\nu_{\max} = 0.3$. These four structures are: unhedged reference model, classical hedged reference model as in Fig. 4, scaled hedged reference model proposed by [6] and the proposed reference model given in Fig. 5. For the scaled case, since reference model has to be slower than the error controller, reference model gain is set to be $k_r = 0.9$, and therefore, the hedging scaling gain is $K_h = 9$.

Pseudo control responses of different structures with P controller to a step input at time $t = 1\,\mathrm{s}$ are given in Fig. 6. The cases with normal hedging and no hedging yield the same pseudo control response. The proposed hedging structure and scaled hedging cases show a response where saturations are mitigated better compared to normal or no hedging cases. Note that, scaled case yields slightly softer response than the proposed structure because of having lower controller gain.

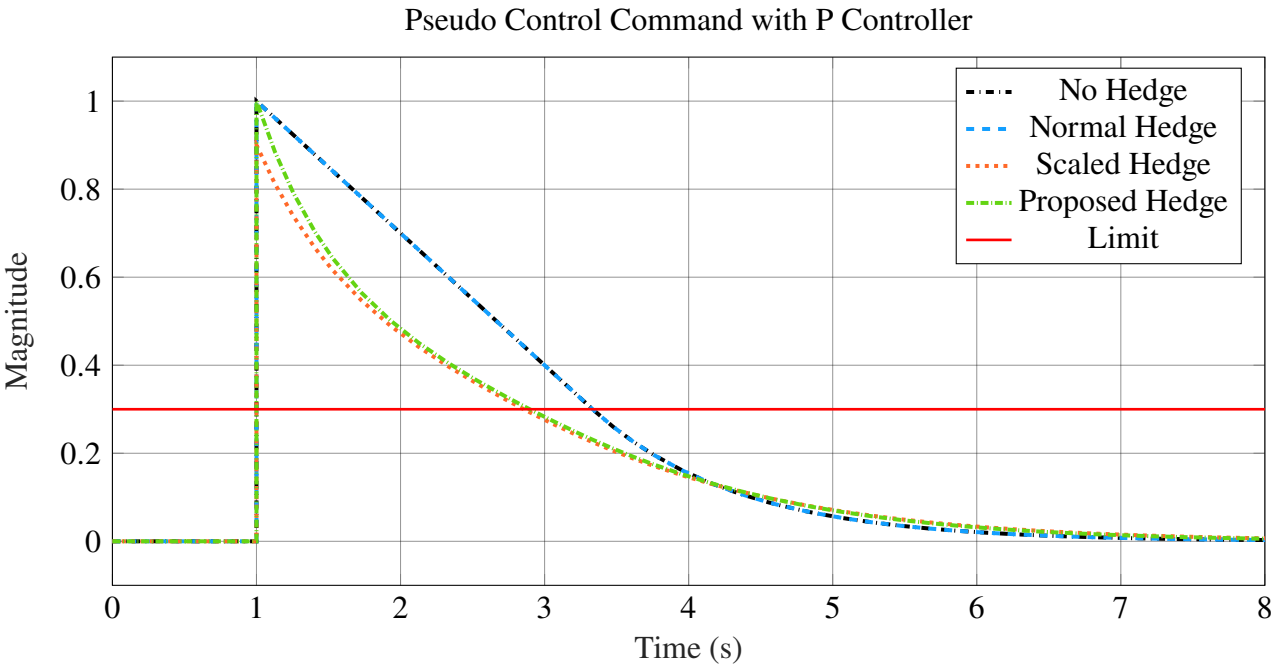

Fig. 6 Pseudo control command ν_{cmd} with different hedging augmentations with P controller.

Tracking responses of different approaches with P controllers are given in Fig. 7. Proposed structure has a better tracking response than no hedging case, whereas normal hedging yields a perfect reference tracking. In the scaled case, since hedging signal is multiplied with a high scaling gain, the reference signal becomes nonphysical, although response is similar to other cases.

Similar analysis is also made for the case with PI controller that has the same bandwidth as P controller. Pseudo control responses with PI controllers are given in Fig. 8. Because of a nonphysical reference signal, the scaled case shows oscillations with PI controller. Proposed structure again shows a command that is decaying faster than the normal hedging case. Fig. 9 shows the tracking responses with PI controller. No hedging case has an overshooting response, while scaled case has slow and oscillating behavior.

Overall, although the proposed structure yields a slightly worse reference tracking response than normal hedging case, it has a better pseudo control response than normal hedging and no hedging cases since the command decays faster in case of saturations. Fast decay of the pseudo control command is favorable in case of saturations, since it decreases the amount of over-command which can also undermine the stability of other axes of the aircraft, as illustrated in the next subsection. Scaled hedging case also provides a similar fast-decaying pseudo control command, while needing the reference model to be slower than the error controller and outputting a nonphysical reference signal, which is undesired in case of an integral action in the controller.

2.3 Quadrotor Example

An example quadrotor simulation to show the effect of different hedging structures is given in this subsection. Simulated quadrotor has a control architecture with attitude control for roll and pitch, and rate control for yaw, along with a vertical velocity control loop. All mentioned controllers are P controllers.

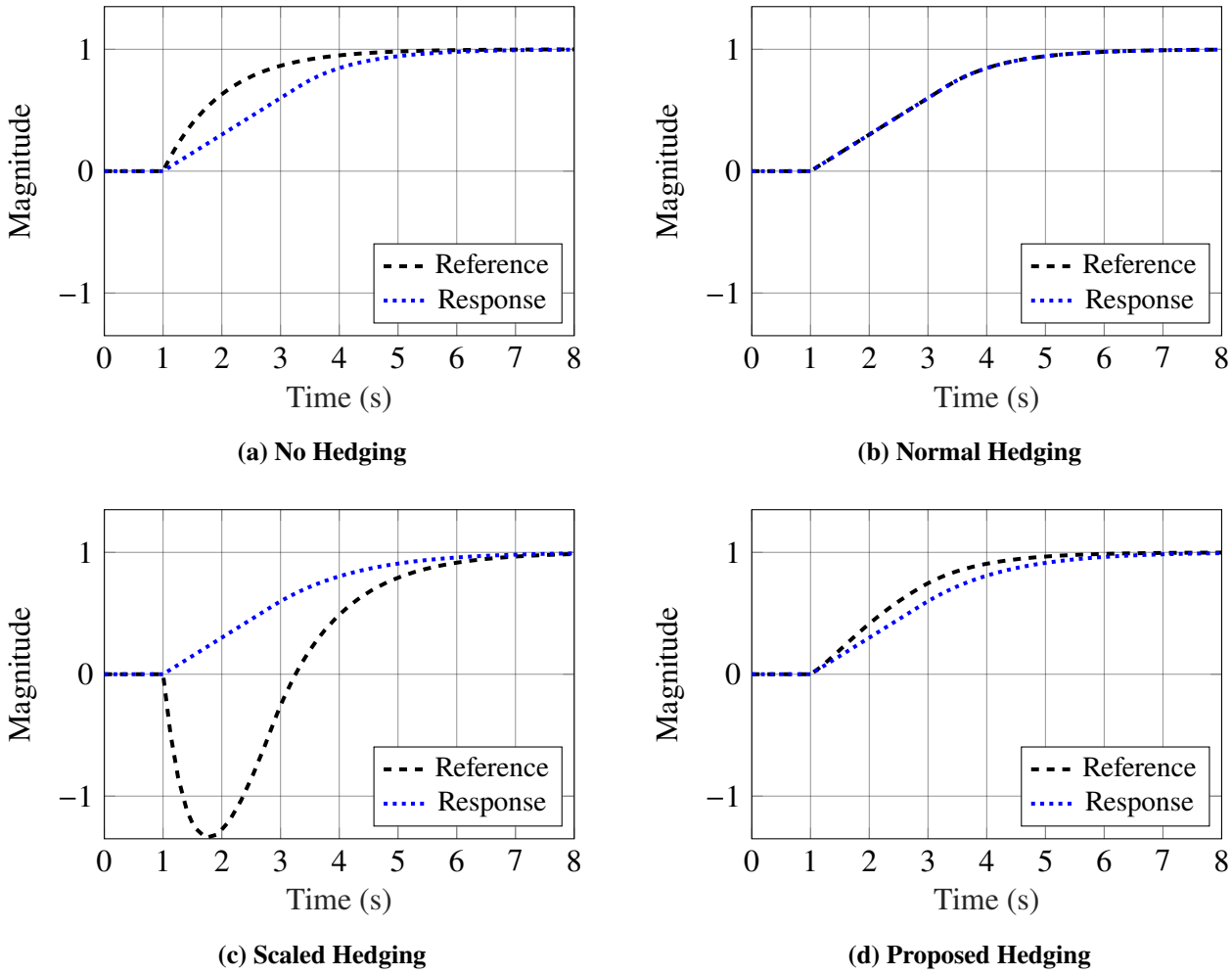

(a) No Hedging **(b) Normal Hedging**

(c) Scaled Hedging **(d) Proposed Hedging**

Fig. 7 Reference signal and response of the system with P controller and different hedging cases.

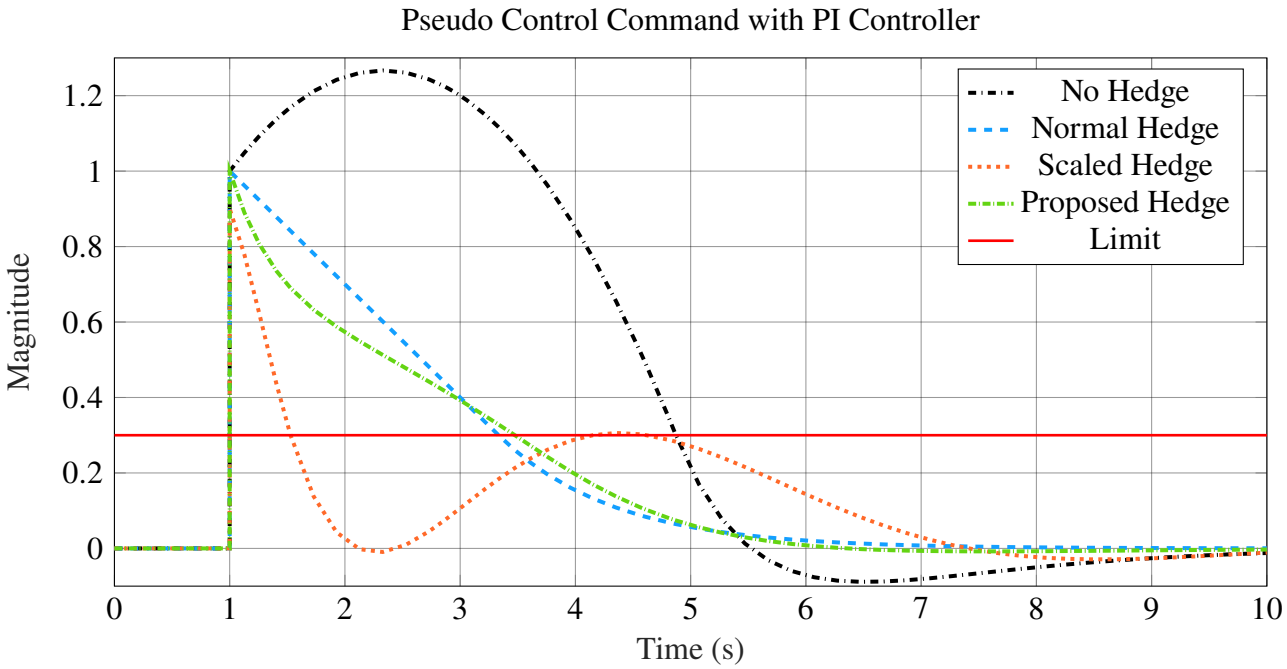

Fig. 8 Pseudo control command ν_{cmd} with different hedging augmentations with PI controller.

A direction-preserving control allocation method, given in [11], is used. The quadrotor is assumed to

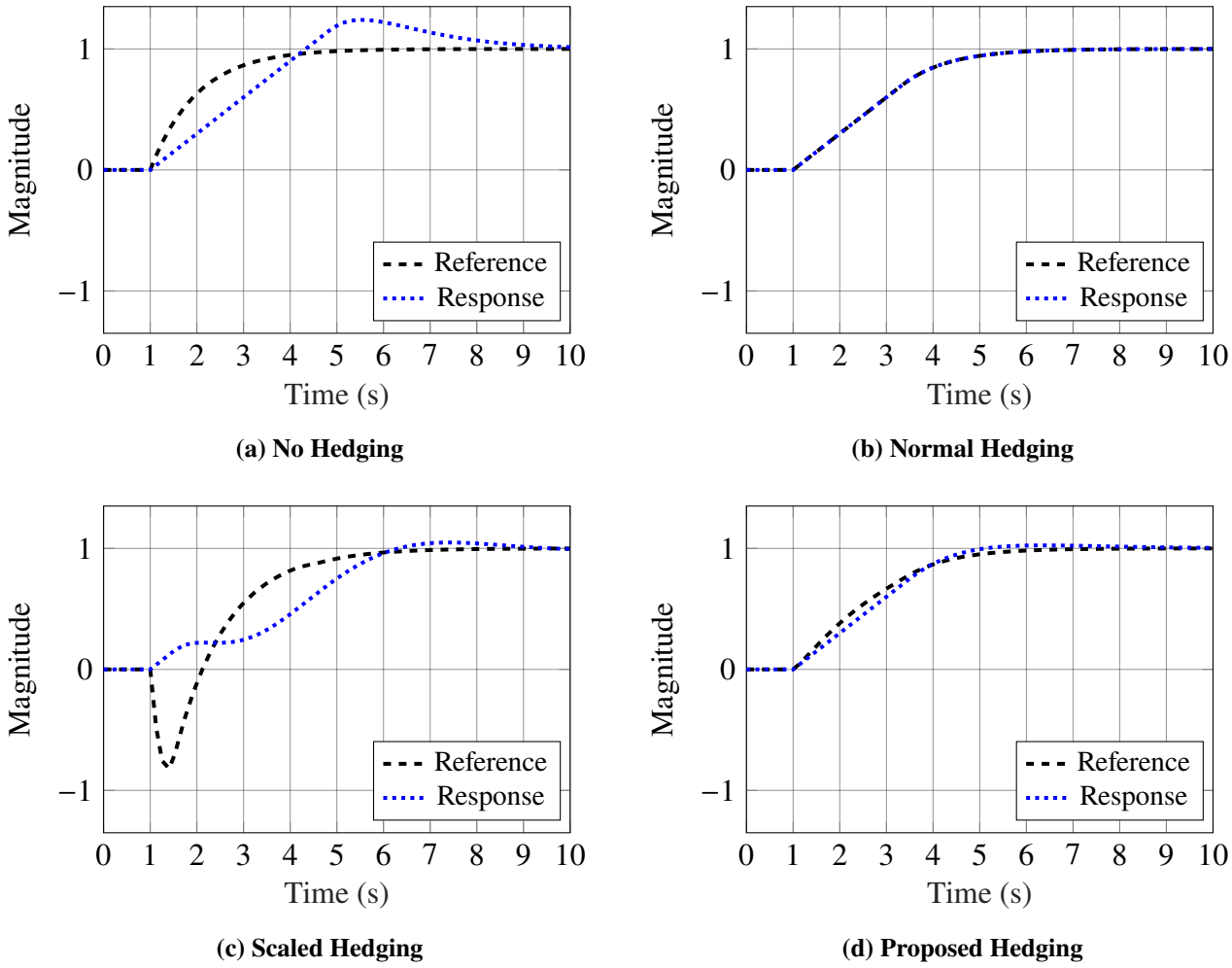

(a) No Hedging

(b) Normal Hedging

(c) Scaled Hedging

(d) Proposed Hedging

Fig. 9 Reference signal and response of the system with PI controller and different hedging cases.

have a low thrust-to-weight ratio of 1.2, and therefore, is prone to saturations. Two different cases are simulated with proposed hedging structure and normal hedging structure.

Yaw rate command and response of the system can be seen in Fig. 10. A step input is given as yaw rate command at time $t = 1\,\text{s}$, with magnitude of $90\,^\circ/\text{s}$. The yaw rate command is set back to zero at $t = 6\,\text{s}$. Note that, response of the aircraft in the proposed and normal hedging cases are nearly identical. During the yaw rate command, roll and pitch angle commands are set to zero. However, because of the severe saturation in yaw axis when the step command is applied, quadrotor's capability of stabilizing itself around the roll and pitch axes is undermined.

Roll and pitch angle responses of the quadrotor are given in Fig. 11 and 12, respectively. It can be seen that, in the normal hedging case, roll and pitch angles deviate significantly from zero, whereas in the proposed hedging case, roll and pitch angles are kept closer to zero. This is because of the faster decay of the pseudo control command in the proposed structure, which results in less over-commanding and therefore, higher authority in roll and pitch axes during saturations. Also note that, during maneuvers without saturations, both hedging structures yield the same responses, which means that the hedging does not alter the nominal closed-loop response.

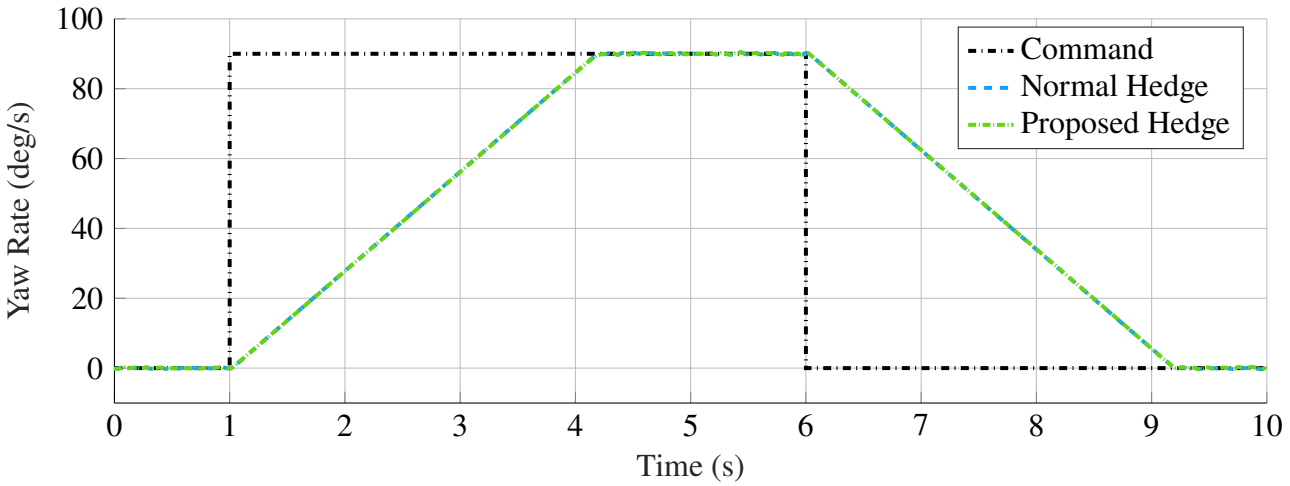

Fig. 10 Yaw rate command and response of the quadrotor with different hedging cases.

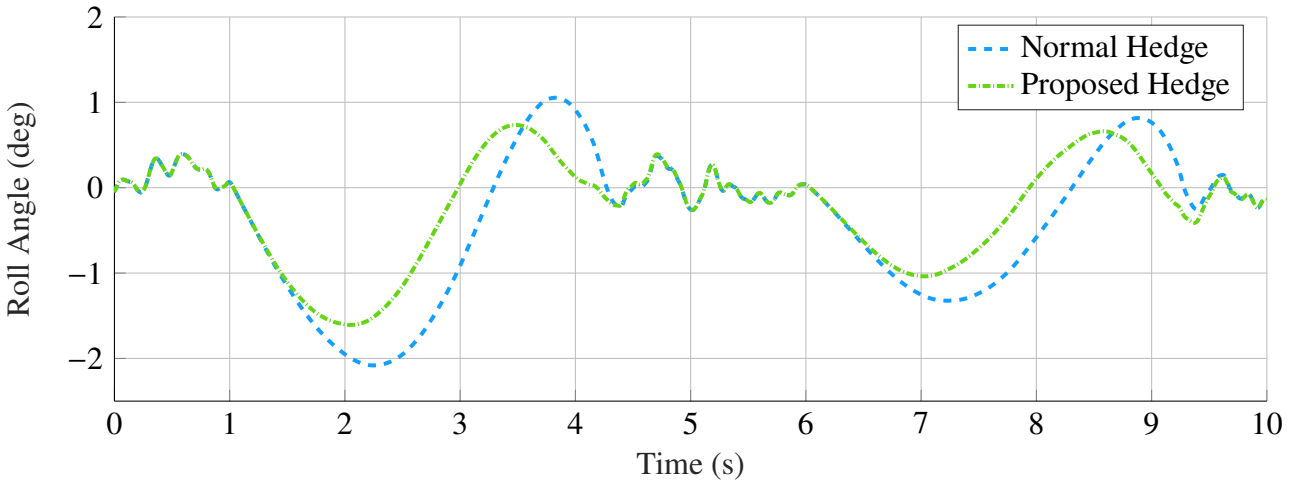

Fig. 11 Roll angle response of the quadrotor with different hedging cases.

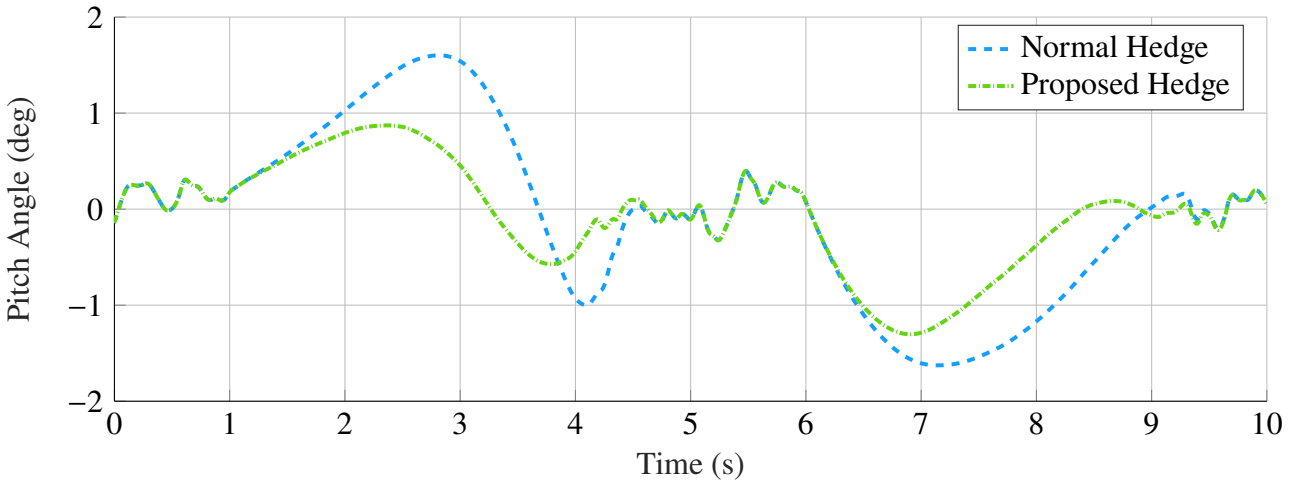

Fig. 12 Pitch angle response of the quadrotor with different hedging cases.

3 Reference Model Architecture for Transition Aircraft

3.1 Flight Control System Architecture

The flight control architecture is given in Fig. 13. The pilot commands are velocities in the control frame, shown with subscript c, which is a local geodetic frame turned by the yaw angle of the vehicle, and a yaw rate. Roll and pitch angle increments are computed through the allocation algorithm by considering them as virtual effectors. Detailed description of the allocation can be found in our previous work [12]. Control architecture consists of velocity, attitude and rate control loops. Each loop contains P controllers, and reference models output translational and angular accelerations feedforwards.

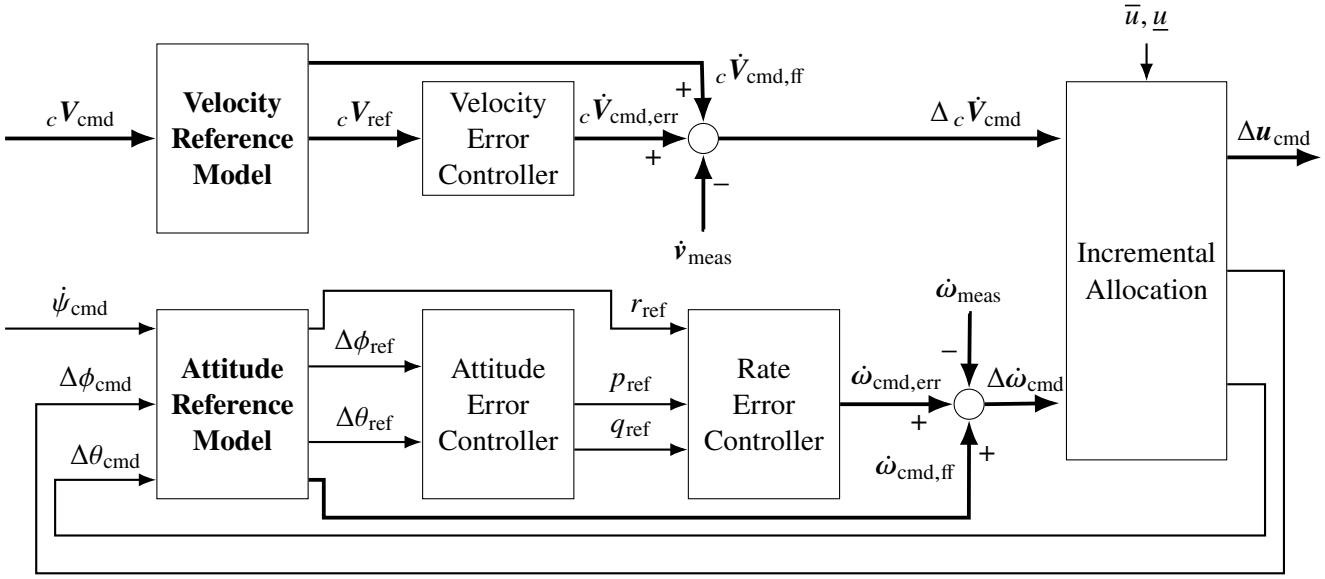

Fig. 13 Flight control system architecture for transition aircraft.

Control loop gains are determined by applying a bandwidth separation between each loop, with a separation factor k. Bandwidth of the velocity loop ω_v is k times slower than the bandwidth of the attitude loop ω_Φ, such that $\omega_v = \omega_\Phi/k$. Similarly, the bandwidth of the attitude loop is k times slower than the bandwidth of the attitude rate loop $\omega_{\dot{\Phi}}$. The bandwidth of the attitude rate is again k times slower than the bandwidth of either the angular acceleration measurement or the actuator bandwidth, whichever is lower. Pseudo control command ν_{cmd} to the allocation consists of linear and angular acceleration increments:

$$\Delta\boldsymbol{\nu}_{\text{cmd}} = \begin{bmatrix} \Delta\,_c\dot{\boldsymbol{V}}_{\text{cmd}} \\ \Delta\dot{\boldsymbol{\omega}}_{\text{cmd}} \end{bmatrix} = \begin{bmatrix} \Delta\,_c\dot{V}_{x,\text{cmd}} \\ \Delta\,_c\dot{V}_{y,\text{cmd}} \\ \Delta\,_c\dot{V}_{z,\text{cmd}} \\ \Delta\dot{p}_{\text{cmd}} \\ \Delta\dot{q}_{\text{cmd}} \\ \Delta\dot{r}_{\text{cmd}} \end{bmatrix}. \tag{11}$$

Resulting pseudo control increment from the allocated effector increments becomes:

$$\Delta\boldsymbol{\nu}_{\text{res}} = B\Delta\boldsymbol{u}_{\text{cmd}} = \begin{bmatrix} \Delta\dot{\boldsymbol{V}}_{\text{res}} \\ \Delta\dot{\boldsymbol{\omega}}_{\text{res}} \end{bmatrix}. \tag{12}$$

Hedging signals that are used by reference models are the difference between commanded and resulting pseudo control increments:

$$\boldsymbol{\nu}_{h,\dot{\boldsymbol{\omega}}} = \Delta\dot{\boldsymbol{\omega}}_{\text{cmd}} - \Delta\dot{\boldsymbol{\omega}}_{\text{res}}, \tag{13}$$

$$\boldsymbol{\nu}_{h,\dot{\boldsymbol{V}}} = \Delta_c\dot{\boldsymbol{V}}_{\text{cmd}} - \Delta_c\dot{\boldsymbol{V}}_{\text{res}}. \tag{14}$$

The control effectiveness matrix for a transition aircraft includes terms with physical actuators and virtual effectors, which are roll and pitch increments, as:

$$B = \begin{bmatrix} \frac{\partial\dot{V}}{\partial\Delta\boldsymbol{\Omega}} & \frac{\partial\dot{V}}{\partial\Delta\boldsymbol{\Phi}} \\ \frac{\partial\dot{\omega}}{\partial\Delta\boldsymbol{\Omega}} & \frac{\partial\dot{\omega}}{\partial\Delta\boldsymbol{\Phi}} \end{bmatrix} = \begin{bmatrix} B_{\dot{V},\boldsymbol{\Omega}} & B_{\dot{V},\boldsymbol{\Phi}} \\ B_{\dot{\omega},\boldsymbol{\Omega}} & \mathbf{0} \end{bmatrix}, \tag{15}$$

where $\boldsymbol{\Omega}$ is the physical actuator commands such as propellers and control surfaces. $\Delta\boldsymbol{\Phi}$ consists of roll and pitch increments, which are called virtual effectors.

3.2 Attitude Reference Model

The attitude reference model is shown in Fig. 14 for pitch and roll angles, where $\boldsymbol{\Phi} = \begin{bmatrix} \phi & \theta \end{bmatrix}^{\mathsf{T}}$. The reference model is second order for roll and pitch because the relative degree is two for attitude. The reference model for yaw rate is first order since the relative degree is one for angular rate. The reference models are tuned, such that $k_{0,\Phi}$ and $k_{1,\Phi}$ are equal to gains of attitude and attitude rate controllers, respectively.

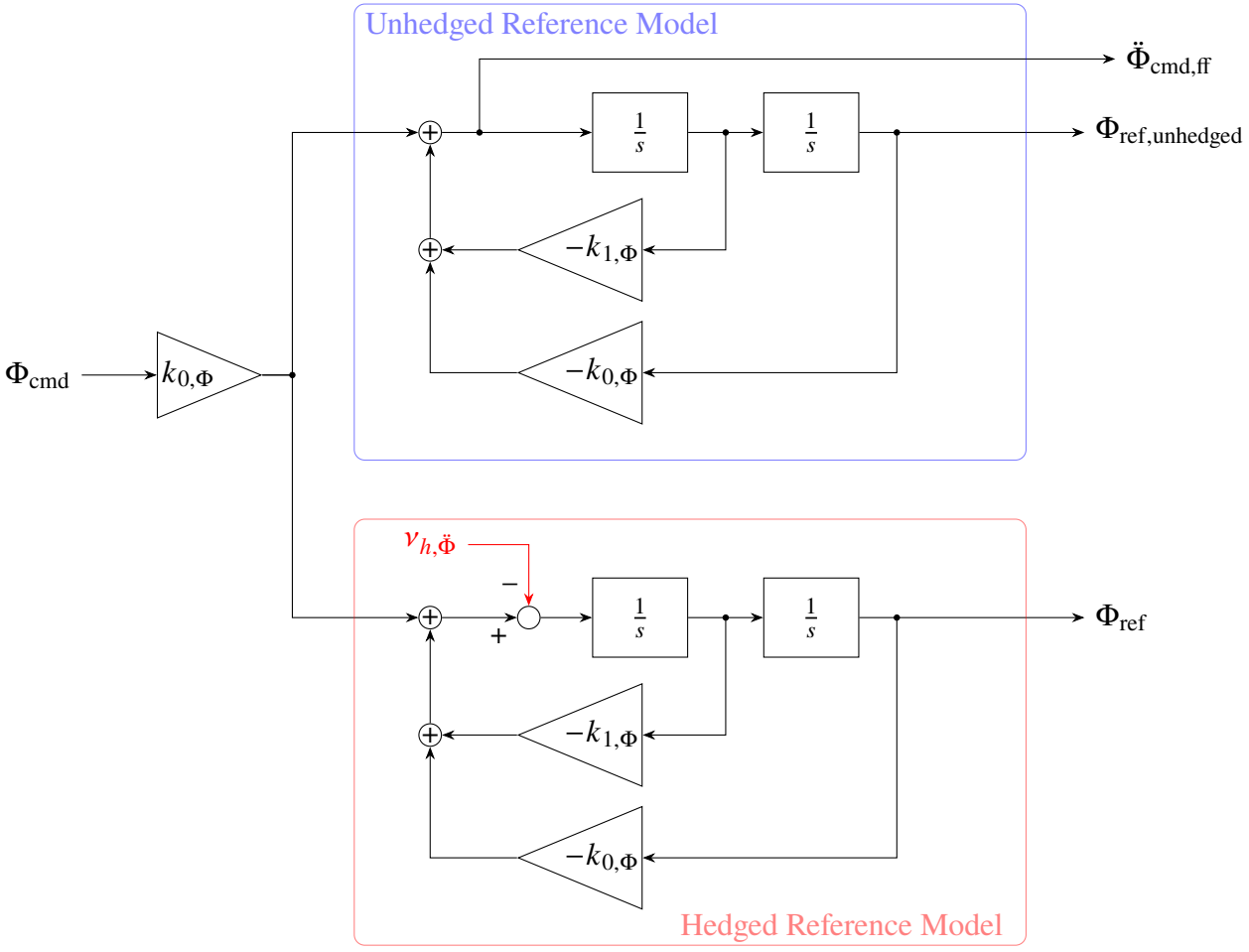

Fig. 14 Attitude reference model.

The hedging signal given in Eq. 13 is the unallocated body angular accelerations. Both the pilot command and reference model output is in Euler angles, therefore, tranformation for the hedging signal is applied:

$$\boldsymbol{\nu}_{h,\ddot{\boldsymbol{\Phi}}} = T_{\boldsymbol{\Phi}b}\boldsymbol{\nu}_{h,\dot{\omega}}, \tag{16}$$

where $T_{\boldsymbol{\Phi}b}$ is the transformation matrix from body angular rates to the derivative of the Euler attitude angles. Note that, Eq. 16 neglects the term $\dot{T}_{\boldsymbol{\Phi}b}\boldsymbol{\omega}$ since the deficiency is only in angular accelerations. The transformation matrix $T_{\boldsymbol{\Phi}b}$ is defined as:

$$T_{\boldsymbol{\Phi}b} = \begin{bmatrix} 1 & \sin(\phi)\tan(\theta) & \cos(\phi)\tan(\theta) \\ 0 & \cos(\phi) & -\sin(\phi) \\ 0 & \sin(\phi)\sec(\theta) & \cos(\phi)\sec(\theta) \end{bmatrix}. \tag{17}$$

The transformation matrix from the Euler attitude rates to body angular rates is the inverse of transformation matrix given above, $T_{b\boldsymbol{\Phi}} = T_{\boldsymbol{\Phi}b}^{-1}$. Then, the feedforward angular acceleration command from reference model $\ddot{\boldsymbol{\Phi}}_{\text{cmd,ff}}$ is transformed from Euler angle accelerations to body frame angular accelerations as:

$$\dot{\boldsymbol{\omega}}_{\text{cmd,ff}} = T_{b\boldsymbol{\Phi}}\ddot{\boldsymbol{\Phi}}_{\text{cmd,ff}} + \dot{T}_{b\boldsymbol{\Phi}}\dot{\boldsymbol{\Phi}}_{\text{ref}}. \tag{18}$$

3.3 Velocity Reference Model

The velocity reference model is shown in Fig. 15. Although the relative degree of velocity control loop is one, the primary source of linear acceleration is tilting, rolling and pitching, which has second order dynamics. Therefore, the underlying dynamics for the velocity control can be assumed to be third order. The reference models for each axis are tuned such that outer-most loop gain $k_{0,V}$ matches the gain of the velocity error controller. Similar to attitude reference model, $k_{1,V}$ and $k_{2,V}$ are tuned such that they are equal to the attitude and attitude rate error controller gains, respectively.

The standard hedging signal for velocity reference models is the unallocated linear acceleration given in Eq. 14. However, attitude is generally the main source of linear acceleration and, from the allocation perspective, it is assumed to be instantaneous. Attitude response of the aircraft can be degraded because of saturation in angular accelerations. Considering only the term $\boldsymbol{\nu}_{h,\dot{V}}$ does not reflect the effect of unallocated angular accelerations on velocity reference models. Therefore, another term is introduced to include such effect of saturations in angular accelerations. For that, the difference between hedged and unhedged attitude references, shown in Fig. 14, is computed as:

$$\boldsymbol{\Phi}_{\text{diff}} = \boldsymbol{\Phi}_{\text{ref,unhedged}} - \boldsymbol{\Phi}_{\text{ref}}. \tag{19}$$

The effect of attitude difference on linear velocities can be computed using their effectiveness shown in Eq. 15:

$$\boldsymbol{\nu}_{h,\boldsymbol{\Phi}\rightarrow\dot{V}} = B_{\dot{V},\boldsymbol{\Phi}}\boldsymbol{\Phi}_{\text{diff}}. \tag{20}$$

Then, the hedging signal is the sum of two terms given in Eq. 20 and Eq. 14 as:

$$\boldsymbol{\nu}_{h,\text{sum}} = \boldsymbol{\nu}_{h,\dot{V}} + \boldsymbol{\nu}_{h,\boldsymbol{\Phi}\rightarrow\dot{V}}. \tag{21}$$

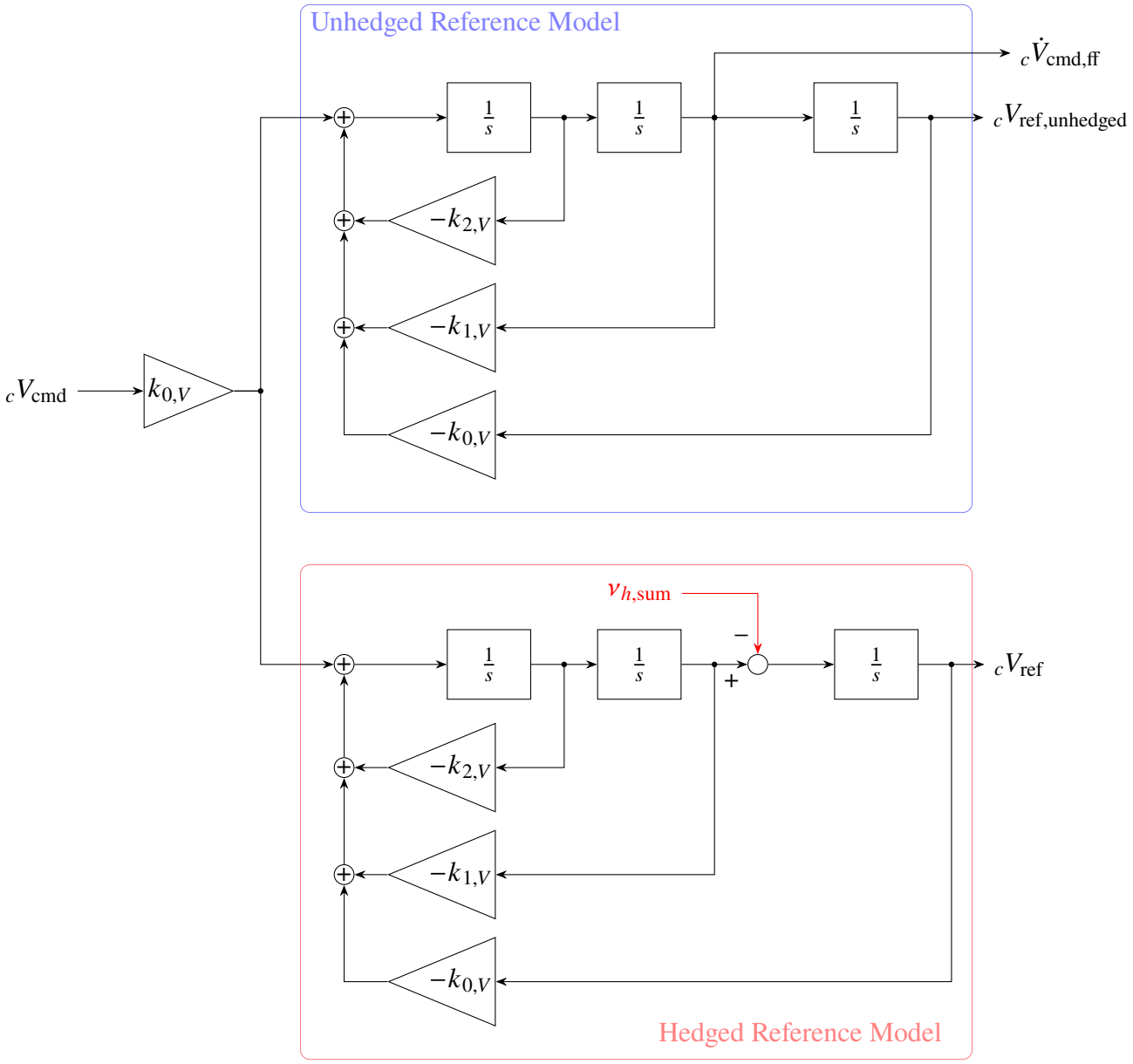

Fig. 15 Velocity reference model.

4 Simulation Results on a Transition Aircraft

The reference models are tested on a nonlinear model of a transition aircraft with eight electrically driven propellers, which are all identical, and wings, shown in Fig. 16. The vehicle has fixed tilt angles and first six propellers are nearly vertical. The rear propellers 7 and 8 are tilted 30°, which means they are acting partially as pushers. Aerodynamic coefficients for the simulation are obtained from wind tunnel experiments and propeller characteristics are obtained from bench tests.

The controller sampling frequency and the simulation update rate are both set to 200 Hz. A pure longitudinal maneuver is simulated, where the vehicle transitions from hover to forward flight at a commanded speed of 21 m/s. The transition maneuver is initiated by a step command in longitudinal velocity, while velocity command in other axes and yaw rate command are kept at zero. The reference signal output from reference models and the vehicle response are shown in Fig. 17. Two different cases are compared, one with hedged reference models and one with unhedged reference models. It can be observed that the response with hedged reference model, with proposed structures in Figs. 14 and 15, tracks the reference velocity closer than the unhedged case. Additionally, a small overshoot is observed in the unhedged case due to the integrative nature of INDI control loops [10].

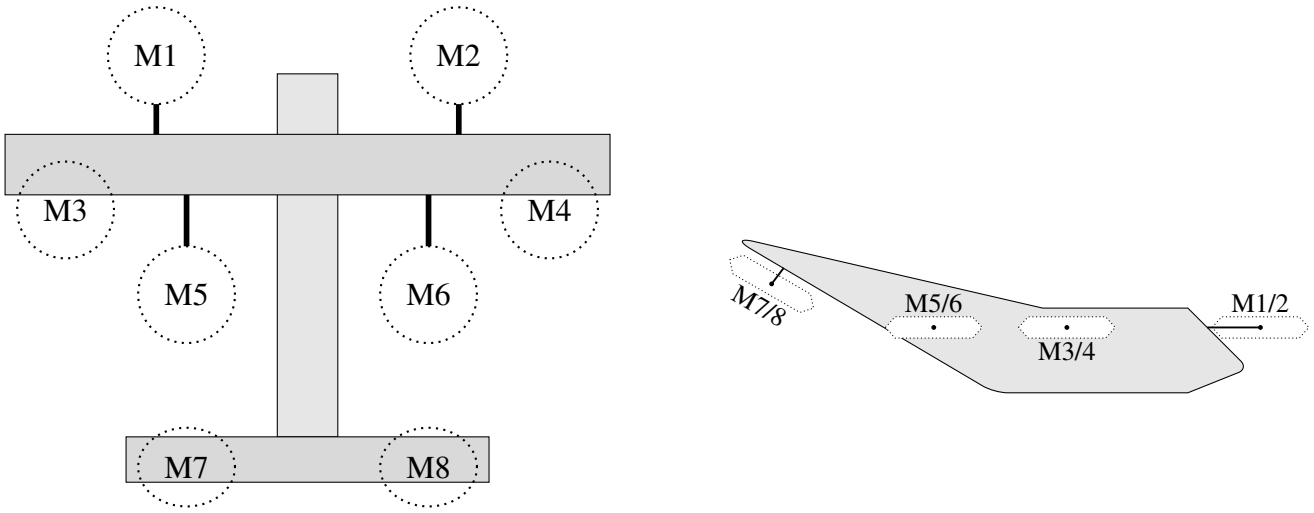

(a) Top view **(b) Side view**

Fig. 16 Vehicle configuration.

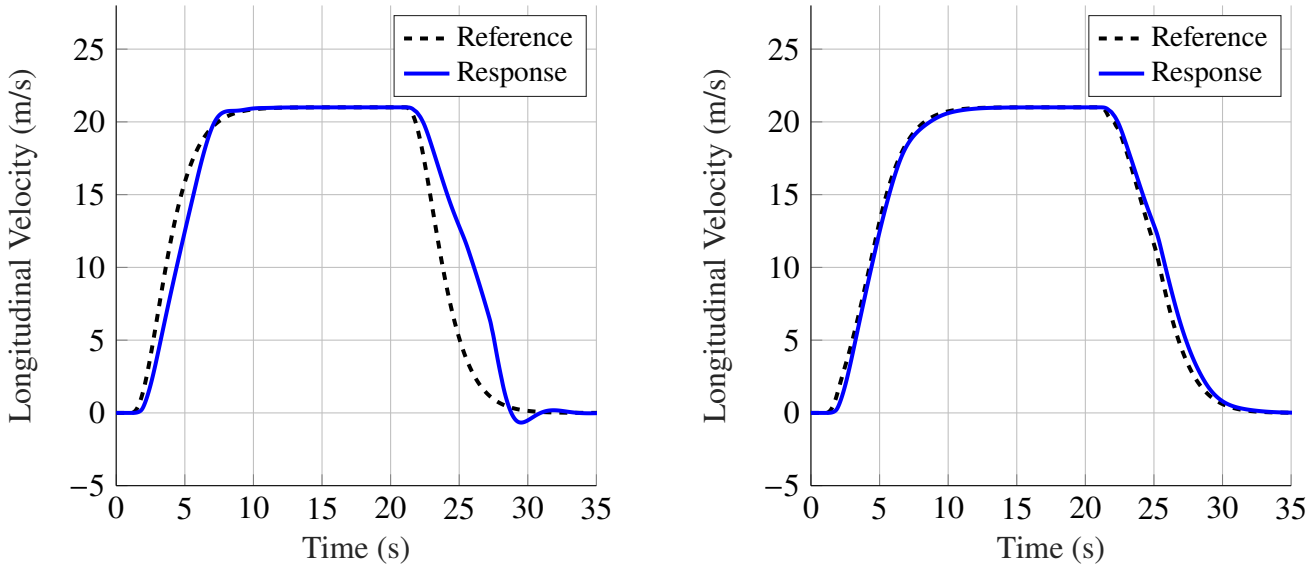

(a) No Hedging **(b) Hedged**

Fig. 17 Reference and response longitudinal velocities with different reference models.

The longitudinal acceleration command ${}_c\dot{V}_{x,\text{cmd}}$ is shown in Fig. 18. It can be observed that the hedged reference model results in a smoother acceleration command, while the response with unhedged reference model has a higher peak, and therefore, it results in a higher over-command.

The pitch angles during the transition maneuver are shown in Fig. 19. Oscillations are observed in the pitch angle response with the unhedged reference model, whereas the attitude response is smoother with the hedged reference model.

5 Conclusions

This paper proposes a linear reference model architecture for a transition aircraft, which makes use of PCH to mitigate the effects of actuator saturation. First, the hedging structures are compared for feedforward-feedback control structures, in terms of the resulting pseudo control command and the reference signal. A structure that generates feedforward command from the unhedged reference model

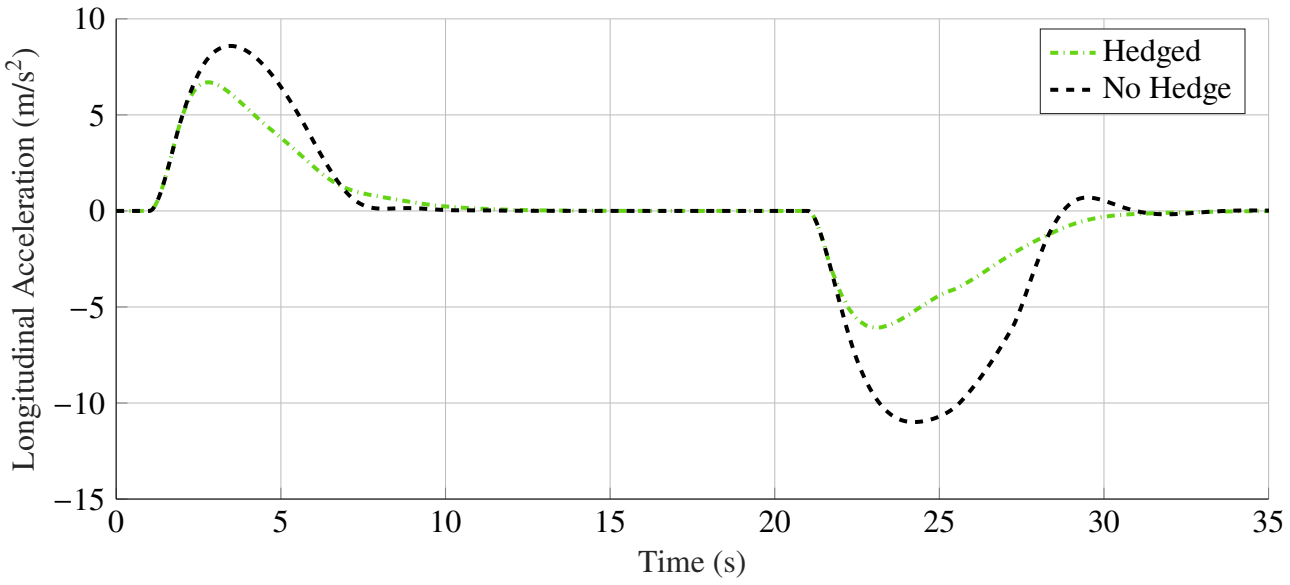

Fig. 18 Longitudinal acceleration commands during transition maneuver with hedged and unhedged reference models.

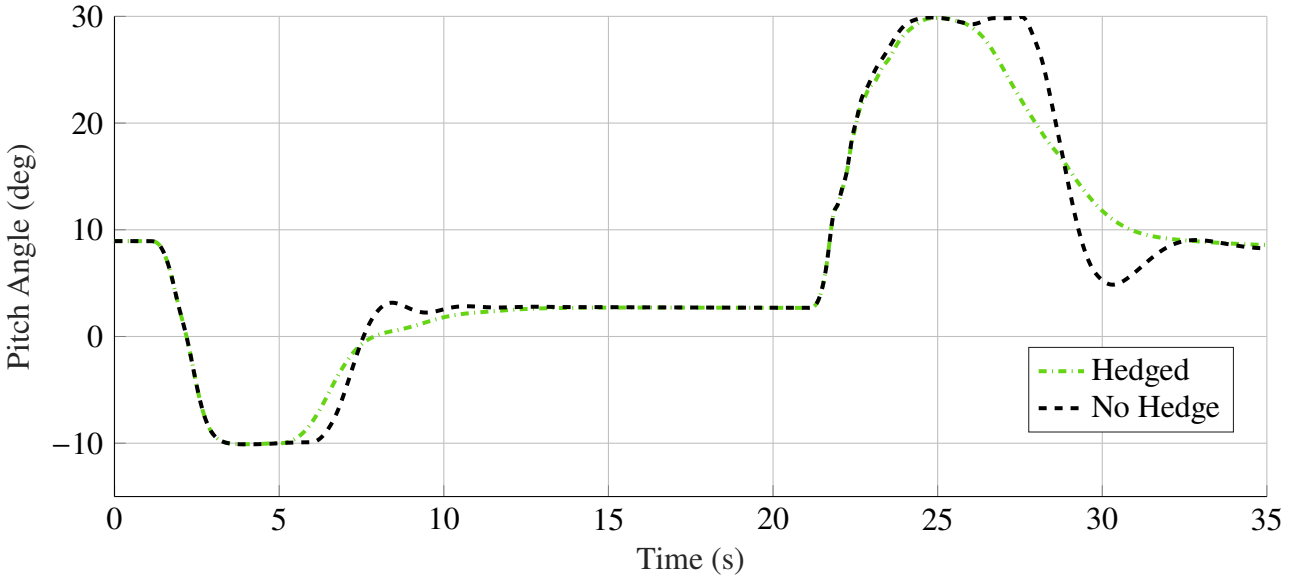

Fig. 19 Pitch angles during transition maneuver with hedged and unhedged reference models.

is found to be advantageous, since the effect of hedging signal on pseudo control command can be observed in a low-pass filtered manner. Then, the reference model architecture for a transition aircraft is presented. The architecture includes velocity and attitude reference models, which are hedged by unallocated linear and angular accelerations. Additionally, since attitude is the main source of linear acceleration, another term is added to the velocity reference model hedging signal to account for the effect of unallocated angular accelerations on linear velocities. Simulation results on a transition aircraft show that the proposed hedged reference model architecture improves tracking performance during a transition maneuver and reduces oscillations, compared to unhedged reference models. It is worth noting that, Pseudo Control Hedging is not sufficient to avoid actuator saturations, since PCH only acts when the saturations occur and mitigates these saturations with a low-pass filtered signal. They can be further avoided with the usage of model information such as flight envelope protections [5, 13].

Acknowledgments

This work is supported by the Bavarian Ministry of Economic Affairs, Regional Development and Energy, through the research program H-AMI 2 in the project AMI-PGS.

Declaration of Use of Artificial Intelligence

Artificial intelligence was not used in the work presented.

References

[1] Eric Johnson and Anthony Calise. Pseudo-control hedging: A new method for adaptive control. In *Advances in Navigation Guidance and Control Technology Workshop*, Alabama, USA, 2000.

[2] Suresh K. Kannan and Eric N. Johnson. Adaptive control of systems in cascade with saturation. In *49th IEEE Conference on Decision and Control (CDC)*, pages 42–47, 2010. doi: 10.1109/CDC.2010.5717276.

[3] Florian Holzapfel. *Nichtlineare adaptive Regelung eines unbemannten Fluggerätes*. PhD thesis, Technische Universität München, 2004. `https://mediatum.ub.tum.de/601905`.

[4] Thomas Lombaerts, Gertjan Looye, Ping Chu, and Jan Albert Mulder. Pseudo control hedging and its application for safe flight envelope protection. In *AIAA Guidance, Navigation, and Control Conference*, 2010. doi: 10.2514/6.2010-8280.

[5] Pranav Bhardwaj, Stefan A. Raab, Jiannan Zhang, and Florian Holzapfel. Integrated reference model for a tilt-rotor vertical take-off and landing transition uav. In *2018 Applied Aerodynamics Conference*. doi: 10.2514/6.2018-3479.

[6] Jiannan Zhang and Florian Holzapfel. Saturation protection with pseudo control hedging: A control allocation perspective. In *AIAA Scitech 2021 Forum*. doi: 10.2514/6.2021-0370.

[7] Ole Pfeifle. *Incremental Control and Allocation for Power-Optimal Flight of Transition Aircraft*, volume 18 of *Fortschrittsberichte des Instituts für Flugmechanik und Flugregelung*. Shaker Verlag, Düren, May 2024. ISBN: 9783844094961.

[8] Li Zhou, Jingtao Yang, Tilman Strampe, and Uwe Klingauf. Incremental nonlinear dynamic inversion based path-following control for a hybrid quad-plane unmanned aerial vehicle. *International Journal of Robust and Nonlinear Control*, 33(17):10304–10327, 2023. doi: 10.1002/rnc.6503.

[9] Agnes Steinert, Stefan Raab, Simon Hafner, Florian Holzapfel, and Haichao Hong. Advancements in incremental nonlinear dynamic inversion and its components: A survey on indi – part ii. *Chinese Journal of Aeronautics*, 38(11):103591, 2025. ISSN: 1000-9361. doi: 10.1016/j.cja.2025.103591.

[10] Agnes Steinert, Stefan Raab, Simon Hafner, Florian Holzapfel, and Haichao Hong. From fundamentals to applications of incremental nonlinear dynamic inversion: A survey on indi – part i. *Chinese Journal of Aeronautics*, 38(11):103553, 2025. ISSN: 1000-9361. doi: 10.1016/j.cja.2025.103553.

[11] Johannes Stephan and Walter Fichter. Fast exact redistributed pseudoinverse method for linear actuation systems. *IEEE Transactions on Control Systems Technology*, 27(1):451–458, 2019. doi: 10.1109/TCST.2017.2765622.

[12] Sinan Çimen and Walter Fichter. Minimum power incremental control allocation using real-time power measurements. In *51st European Rotorcraft Forum*, 2025.

[13] Jurian Stougie, Tijmen Pollack, and Erik-Jan Van Kampen. Incremental nonlinear dynamic inversion control with flight envelope protection for the flying-v. In *AIAA SCITECH 2024 Forum*. doi: 10.2514/6.2024-2565.